

A FRACTAL AND LONG-RANGE CORRELATION ANALYSIS OF PLANT NUCLEUS ULTRASTRUCTURE

V.V. MORARIU*, C. CRĂCIUN**, SILVIA NEAMȚU*, L. IARINCA*, C. MIHALI**

*Department of Molecular and Biomolecular Physics, National Institute for R&D of Isotopic and Molecular Technology, P.O. Box 700, Cluj-Napoca 5, 400293, Romania

**Faculty of Biology, "Babeș-Bolyai" University, Cluj-Napoca, Romania

Abstract. Transmission electron microscopy images of nuclei from leafs of *Lycopersicon esculentum*, *Capsicum annum*, *Tagetes patula* and *Calendula officinalis* were characterized by fractal dimension D of the images. The mean value of D was 1.664 ± 0.020 , which did not appear to be influenced by the age of the plant. Correlation analysis was performed on selected profiles across nuclei by detrended fluctuation analysis (DFA) and Fast Fourier Transform (FFT). Profiles across euchromatin regions proved to be characterized by short-range correlations extending over medium range distances. On the other hand profiles of the same nuclei crossing nucleolus, heterochromatin and euchromatin regions were characterized by long-range correlation having a mean DFA correlation exponent $\alpha = 1.22 \pm 0.032$. The spectral exponent proved to be controlled by significant trends and therefore it was of not much use.

Key words: ultrastructure, nucleus, nuclear chromatin, fractal dimension, long-range correlation, short-range correlation.

INTRODUCTION

The fractal and the long-range correlation analysis of biological structures has been a constant subject ever since Mandelbrot's famous essay [11]. A major interest was focused on the fractal properties of nuclear chromatin especially for diagnosis purpose. Most of the investigations have been performed on mammalian nuclear chromatin. This kind of analysis represents a quantitative evaluation of an image in addition to the qualitative visual assessment of its content. Many examples refer to the investigation of cancer cells [2–4, 7, 8, 12–15, 17].

The general goal of the present work was to explore the basic characteristics of the vegetal nucleus ultra structure in order to build up reference characteristics for further studies. The cell nuclei images of four different species of plants at three different ages were investigated by using fractal dimension D and long-range correlation characteristics.

Received July 2006;
in final form October 2006.

The fractal dimension, D , of a profile or surface is a roughness measure [5]. Higher values indicate rougher surface. Fractal dimension is regarded as *local* property of the system. This is in contrast to the long-range correlation property of the system, which is a *global* property. Information about the long-range correlation can be obtained from various methods of fluctuation analysis such as Fast Fourier Transform (FFT), detrended fluctuation analysis (DFA). In principle, fractal dimension and long-range correlation are independent of each other [5]. The two notions are closely linked in self-affine processes where the local properties are reflected in the global ones. The standard method to assess the long-range correlation is to calculate the Hurst coefficient. However the calculation can be done on stationary data only while in our case, we deal with non-stationary data as further shown in the text.

The structure of a nucleus is known to be quite heterogeneous: it contains at least a nucleolus and patches of heterochromatin, which are relatively dark, compact structures. They are scattered in a less dense volume of euchromatin. The ensemble of the nucleus structure is well suited for fractal dimension analysis of the image. Long-range correlation analysis involves selection of profiles across the nucleus image and the subsequent analysis of the corresponding series of gray values. We selected several profiles in each nucleus such as to cross all kinds of substructures including euchromatin, heterochromatin and nucleolus. The series of data were subjected to FFT and DFA. It was considered of further interest to investigate the correlation characteristics of the euchromatin itself so that profiles were selected such as to cross only euchromatin regions.

MATERIALS AND METHODS

Two species of economic interest (tomato – *Lycopersicon esculentum* and green pepper – *Capsicum annuum*) and two plants (*Tagetes patula* and *Calendula officinalis*) of the spontaneous flora have been selected. Plants were grown in pots under artificial light and constant temperature in the lab. Tissue fragments were collected from the median zone of the foliar limb, located at middle level of the plant. The age of the plants was 24–33 days, 65–66 days and 6 months respectively. The tissue fragments were treated in a 2.7% glutaraldehyde solution and washed four times in 0.15M buffered phosphate at pH 7.2. Then the tissues were fixed in a 1% osmic acid solution followed by dehydration with acetone of increasing concentrations. Finally the samples were infiltrated in a synthetic resin (Durcupan) and thin sections were cut with a LKB_III ultra microtome. The thin sections were contrasted with uranyl acetate and lead citrate solutions. Finally they were examined by a Jeol JEM 1010 transmission electron microscopy.

The images were analyzed by using IMAGE-J software [1, 16]. The general aspect of the nuclei including nucleolus, euchromatin and heterochromatin was characterized by the fractal dimension of the image. The method basically relies upon the box counting method, which is applied after preliminary applying a

threshold to the image [1, 16]. Fractal dimension of an image is regarded as a local property of the image [5].

The euchromatin structure was characterized by selecting profiles in the nucleus, which avoided dense structures such as nucleoli or patches of heterochromatin. In a similar manner profiles were selected such as to cross all the features of a nucleus including nucleolus, heterochromatin and euchromatin. The profiles were analyzed for long-range correlation as described below.

The profiles were selected and read by the IMAGE-J software then the data were transferred to ORIGIN and further subjected to FFT and DFA. The DFA method was run on our own software. The methods were previously checked against series of data with established characteristics [9]. The spectral analysis resulted in the so-called β long-range correlation exponent, which is the slope of the double logarithmic plot of the spectrum. The exponent is $\beta = 0$ for a random uncorrelated series and $\beta = 2$ for a Brownian noise. This method is valid for stationary series of data. Many real series of data have non-stationary characteristics. The correlation exponent β , in such a case, reveals the overall correlation of the data, which may be due to two contributions: one, which represents correlation of the fluctuation and another due to trends. The value of β for a straight line (a trend) for example is close to 2. A trend superposed on correlated fluctuation may result in a β value, which tends to a limiting value of 2, depending on the weight of trend. The problem which may arise is that very often the trend may dominate the long-range correlation exponent β so that its value does not reflect the correlation of the fluctuation in the data. This is why it is essential to decide whether the series is stationary or non stationary and therefore establish what kind of analysis is suitable for characterizing the correlation. DFA method has the advantage that it can remove trends and therefore offers the possibility to characterize the correlation of the stationary fluctuation. The result of DFA is α exponent, which describes the long-range correlation of the detrended series. Its value is $\alpha = 0.5$ for a random uncorrelated series, $\alpha = 1.5$ for a Brownian noise and $\alpha < 0.5$ for anti correlation. A simple way to check up the non-stationary character of the series of data is to first determine the experimental value of β and α exponent from the actual series of data. It is known that for a stationary series of data the two exponents are related by $\beta = 2\alpha - 1$ [6]. If this relationship is not obeyed then the series is non-stationary. This further means that only α exponent offers a reliable measure of the fluctuation correlation.

RESULTS AND DISCUSSION

An example of nucleus structure subjected to fractal dimension and correlation analysis respectively is illustrated in Fig. 1. Also the profiles selected

for the correlation analysis are included in the figure. The fractal dimension D of images is included in Table 1. Two images of each case were selected for analysis. The fractal dimension varied in the 1.5–1.8 range with a mean value of $D = 1.664 \pm 0.02$ and a Gaussian distribution centered at 1.673. Further analysis of these data also shows that the ranking plot can be described by an exponential growth (not shown). Unfortunately, at the time of the experiment the number of images was restricted by the project so that a vast statistical analysis was not possible.

Table 1

Fractal dimension of the leaf cell nuclei at various ages

No	Species	Age of the plant	Description of the nuclei	Fractal dimension
1	Lycopersicon esculentum (Tomato)	24 days	Normal structure; Nuclei with uniform outline	1.623 1.613
2		66 days	Normal structure; Nuclei with uniform outline	1.669 1.673
3	Capsicum annuum (Green pepper)	24 days	Normal structure	1.620 1.736
4		66 days	Hyper chromatin	1.666 1.776
5		6 months	Hyper chromatin	1.699 1.585
6	Tagetes patula	33 days	Normal structure	1.721 1.677
7		6 months	Abnormal acicular structures Abnormal caryoplasma Abnormal nucleolus	1.694 1.741
8	Calendula officinalis	33 days	Normal structure; additional hypertrophic nucleolus	1.661 1.509
9		65 days	Euchromatin is dominant Hypertrophic nucleolus	1.865 1.563 1.521

There is a slight tendency of D to increase with the age but this effect does not seem to be visible for *Callendula officinalis*. Nevertheless, the visual difference among images proved to be rather modest. The statistics did not allow uncover second order effects such as the effect of age of the plant. On the other hand, the work represented the basic step towards investigating physical effects on nuclei ultra structure which are expected to be more pronounced. Features which might affect the fractal dimension in our case are: nucleoli dimension and shapes, the dimension and shape of heterochromatin patches, the shape of nuclei, the presence of abnormal bodies within the nuclei etc. The fractal dimension is possibly mildly sensitive to the aging process of the plant. Its range of values further tells that the nuclei are relatively non-uniform structures.

It is interesting to mention that the range of fractal dimension values noticed in this work falls within similar values for example to human breast cancer cells [2]. Cited paper reported a significant reduction of the fractal dimension during induced apoptosis. On the other hand higher values were reported for benign and malignant breast epithelial cell nucleus which had a fractal dimension around 2.5 [3]. Also the local fractal dimension in HeLa cells proved to be within a similar range (2.2 – 2.6) [18].

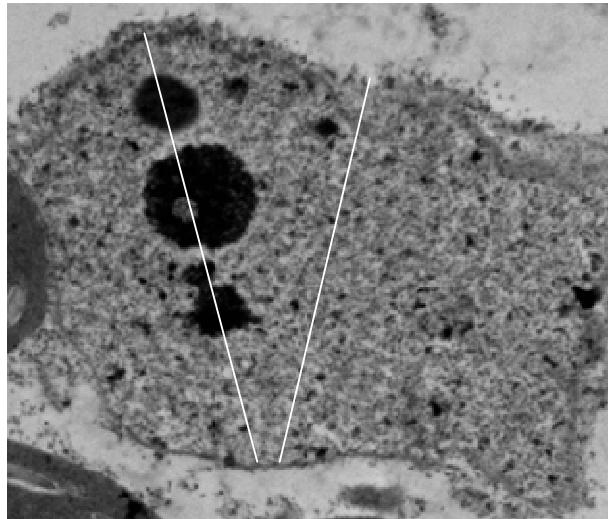


Fig. 1. An electron transmission microscope image of a nucleus of *Lycopersicon esculentum*. The long-range correlation of the chromatin was estimated from the profile crossing the nucleoli on the left side while the correlation of euchromatin from the profile on the right side.

Next we discuss the results concerning the correlation properties of selected profiles across nucleus ultra structure. A large part of the nuclei is represented by the euchromatin content which appears as a relatively uniform structure yet with visible details. We thought to be of interest to explore the correlation property of this nuclear component as compared to the correlation characteristics of all features contained by the nucleus. An example (for *Lycopersicon esculentum*) of gray values profile across euchromatin (Fig. 2), its spectrum (Fig. 3) and the corresponding DFA plot (Fig. 4) are shown below.

The spectrum (Fig. 3) is described by a power law with a correlation exponent $\beta \approx 2$. This value at the upper limit of a Brownian noise clearly can be suspected of a major contribution to the correlation by the trend in the series. This has already been noticed in Fig. 2 where the trend is illustrated by the linear fitting of the data. The usual solution is to use DFA, which removes the trend. The result is illustrated

in Fig. 4. DFA shows a non-linear plot (Fig. 4), which suggests that there is no long-range correlation along the selected profile of euchromatin. A long-range correlation needs a linear plot over at least two orders of magnitude. In fact the data show a short-range correlation which does not extend beyond an order of magnitude.

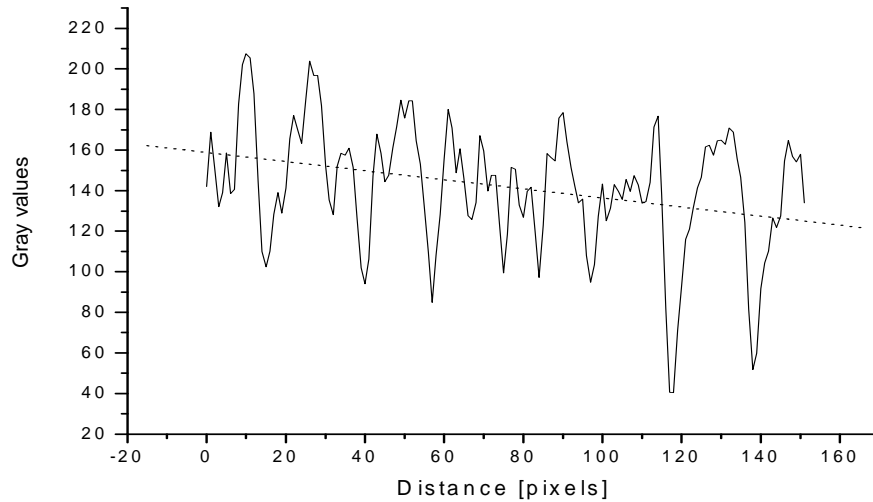


Fig. 2. Gray values of a profile across euchromatin of a nucleus from the leaf of *Lycopersicon esculentum*. The trend (non stationary characteristic) is illustrated by the straight fitting line.

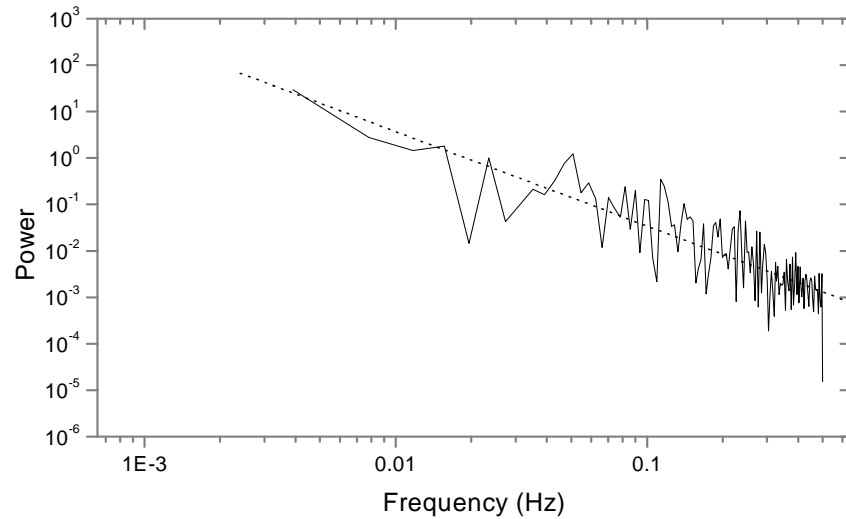


Fig. 3. Spectrum of the series illustrated in Fig. 2. The slope of the fitting line is the apparent long-range correlation exponent $\beta = 2.03$. Although the series appears as quasi-periodic (Fig. 2) the spectrum is of $1/f^\beta$ type.

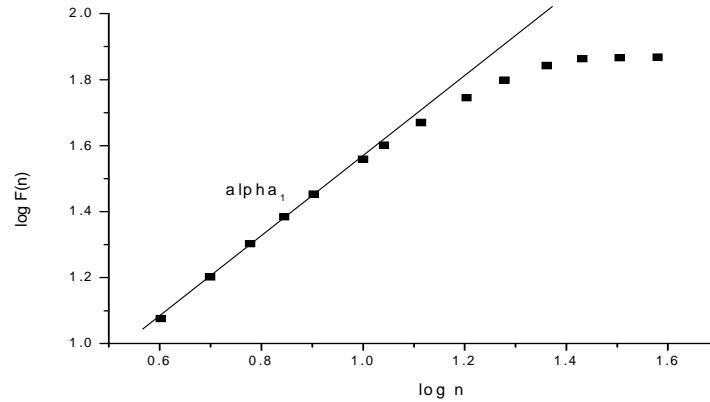


Fig. 4. Detrended Fluctuation Analysis of a profile through euchromatin illustrated in Fig. 2 above.

This kind of analysis was applied to various selected profiles ($n = 20$) for all nuclei listed in Table 1. The slope of the linear fit of the lower part of the plot was α_1 . The distribution of α_1 was Gaussian (not shown) with a median value at $\alpha_1 = 1.1$ and a width of the distribution $w = 0.291$. The mean value was 1.072 ± 0.04 . It appeared that α_1 was not sensitive to the age of the plant.

Further, we analyzed selected profiles of the chromatin structure that included nucleolus, heterochromatin and euchromatin. A similar set of examples is given below for the same nucleus as in Fig. 1.

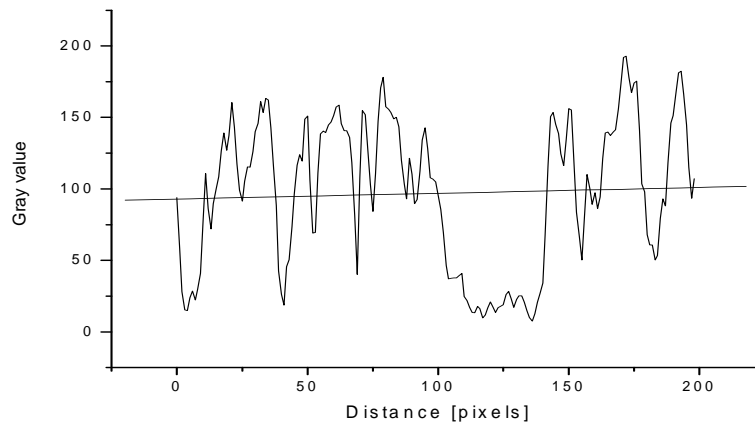


Fig. 5. Profile across chromatin of the same nucleus as shown for euchromatin in Figures 2–4. The wider gap in the plot corresponds to the dark region of nucleolus. The straight fitting line with a nonzero slope suggests the presence of a trend in the data although the real trend can be more complicated than this approximation.

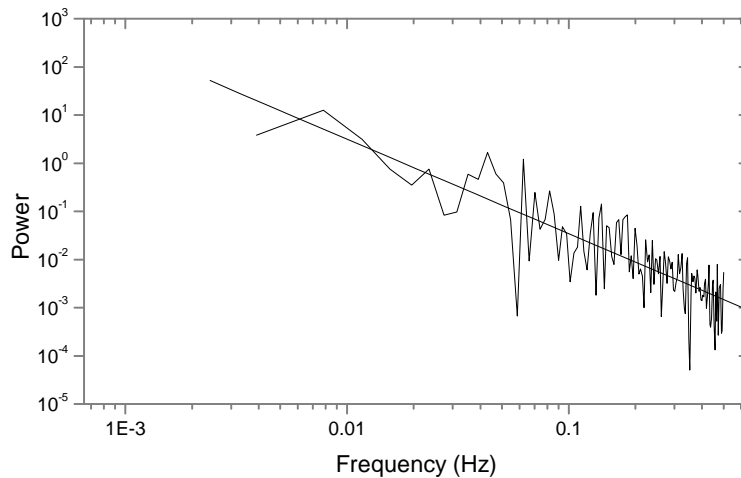


Fig. 6. Spectral analysis of the profile illustrated in Fig. 4. The slope of the plot i.e. the long-range correlation exponent is $\beta = 1.962 \pm 0.121$. This high value and the trend illustrated by Fig. 4 suggest that the series is non stationary therefore the value of β does not provide useful information about the correlation of fluctuation. Instead it is dominated by the correlation imposed by the trend.

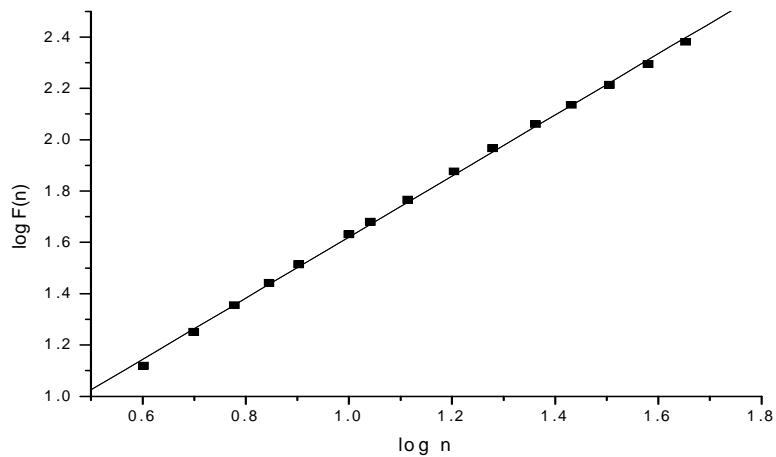


Fig. 7. Detrended Fluctuation Analysis of the profile illustrated in Fig. 4. The long-range correlation exponent is $\alpha = 1.191 \pm 0.011$.

Fig. 7 shows that the chromatin profile is characterized by a long-range correlation and this proved to be true for most of the chromatin structures from various nuclei listed in Table 1. The analysis of the example presented in Figures 5–7 clearly show that the series of data is non stationary. The value of β is 1.962

and $\alpha = 1.191$ (Figs. 6–7). Therefore, $2\alpha - 1 = 1.382$. As $\beta \neq 2\alpha - 1$, it results that the series is non-stationary and only α exponent is a true measure of the fluctuation correlation. Further, the DFA analysis shows that the profile across chromatin structures is long-range correlated. The mean value of the long-range correlation exponent for the chromatin of various nuclei is $\alpha = 1.22 \pm 0.032$. All the mean values are summarized in Table 2. There is no available data in the literature to compare the present results for similar species. In a study on breast epithelial cells, the scaling exponent on chromatin varied between 0.5 and 0.8 for benign samples and between 0.4 and 0.7 for malign cases [4]. These figures revealed significant differences among the long-range correlation exponents of plant and animal chromatin, respectively.

Table 2

Mean values of the fractal and correlation characteristics of studied nuclei

Property	Mean value	Observation
Fractal dimension of nuclei	1.664±0.02	–
Correlation characteristic of chromatin*	1.22±0.032	Long-range correlation
Correlation characteristic of euchromatin*	1.072±0.04	Short-range correlation

* It refers to the correlation exponent resulting from DFA.

In conclusion, we have characterized the mean values of the fractal dimension of studied nuclei as well as the correlation characteristics of euchromatin and heterochromatin. These will represent reference data for further studies concerning physical influences on the plants such as changes induced by the exposure to zero magnetic field environment. As the exposure led to obvious aging of nuclei, it is expected that changes could be quantified by the methodology presented in this work.

Acknowledgements. This paper is part of a project supported by the Romanian Scientific Research Agency.

REFERENCES

1. ABRAMOFF, M.D., P.J. MAGELHAES, S.J. RAM, Image processing with Image-J, *Biophotonics International*, 2004, **11**, 36–42.
2. CASTELLI, C., G.A. LOSA, Ultrastructural complexity of nuclear components during early apoptotic phases in breast cancer cells, *Anal. Cell. Pathol.*, 2001, **23**, 1–9.
3. EINSTEIN, A.J., HAI-SHAN WU, JUAN GIL, Self-affinity and lacunarity of chromatin texture in benign and Malignant Breast Epithelial Cell Nuclei, *Phys. Rev.Lett.*, 1998, **80**, 397–400.
4. EINSTEIN, A.J., HAI-SHAN WU, JUAN GIL, Detrended fluctuation analysis of chromatin texture for diagnosis in breast cytology, *Fractals*, 2002, **10**, 19–25.
5. GNEITING, T., M. SCHLATHER, Stochastic models that separate fractal dimension and the Hurst effect, *SIAM Review*, 2004, **46**, 269–282.

6. GOLDBERGER A.L., L.A.N. AMARAL, L. GLASS, J.M. HAUSDORFF, P.C. IVANOV, R.G. MARK, J.E. MIETUS, G.B. MOODY, C-K. PENG, H.E. STANLEY, Physiobank, physiokit, and physionet: components of a new research resource for complex physiologic signals, *Circulation*, 2000, **101**: e215–e220.
7. HAMILTON, P., K. DILLON, P. BARTELS, J. DIAMOND, D. THOMPSON, D. ALBERTS, Chromatin texture analysis of histologically normal colorectal mucosa in patients with adenomatous polyps and colorectal cancer, *ISAC XX International Congress Abstracts*, 2000.
8. LEBEDEV, D.V., M.V. FILATOV, A.I. KUKLIN, A.KH. ISLAMOV, E. KENTZINGER, R.PANTINA, B.P. TOPERVERG, V.V. ISAEV-IVANOV, Fractal nature of chromatin organization in interphase chicken erythrocyte nuclei: DNA structure exhibits biphasic fractal properties, *FEBS Lett.*, 2005, **579**, 1465–8.
9. LOSA, G.A., C. CASTELLI, Nuclear patterns of human breast cancer cells during apoptosis: characterization by fractal dimension and co-occurrence matrix statistics, *Cell&Tissue Res.*, 2005, **322**, 257–267.
10. MORARIU, V.V., O. ZAINEA, A. BENDE, O. POPESCU, The statistical physics of microbial genomes: part I. Organization of coding sequences in the chromosome of *Escherichia coli*, *Rom. J. Biophys.*, 2006, **16(2)**, 103–110.
11. MANDELBROT, B., *The fractal geometry of nature*, W.H. Freeman, New York, 1982.
12. NAFE, R., B. YAN, W. SCHLOTE, B. SCHENIDER, Application of different methods for nuclear shape analysis with special reference to the differentiation of brain tumors, *Anal. Quant. Cytol. Histol.*, 2006, **28**, 69–77.
13. NIELSEN B, F. ALBREGTSEN, H.E. DANIELSEN, The use of fractal features from the periphery of cell nuclei as a classification tool, *Anal. Cell. Pathol.*, 1999, **19**, 921–37.
14. NIWA, Y., T. YOSHIDA, K. MORIWAKE, T. OKAMOTO, C. KURAMOTO, E. YAMAZ, Determination of fractal dimension using digital nuclear image of lymphocyte, *Rinsho Byori*, 2002, **50**, 702–705.
15. RANDALL, A., R.C. SILVA, F.G. PEREIRA, N.J. LEITE, I. LORAND-METZE, K. METZE, The fractal dimension of nuclear chromatin as a prognostic factor in acute precursor B lymphoblastic leukemia, *Cellular Oncology*, 2006, **28**, 55–59.
16. RASBAND, W.S., Image-J, U.S. National Institutes of Health, Bethesda, Maryland, USA, <http://rsb.info.nih.gov/ij/>, 1997–2005.
17. SABINO, D.M.U., L.F. COSTA, S.L.R. MARTINS, R.T.CALADO, M.A. ZAGO, Automatic leukemia diagnosis, *Acta Microscopica*, 2003, **12**, 1–6
18. TOTH, K., T.A. KNOCH, M. WACHSMUTH, M. FRANK-STOHR, M. STOHR, C.P. BACHER, G. MÜLLER, K. RIPPE, Trichostatin A-induced histone acetylation causes decondensation of interphase chromatin, *Journal of Cell Science*, 2004, **117**, 4277–87.